Academic Journal of International University of Erbil

Journal Homepage: https://ojs.cihanrtv.com/index.php/public

PRINT-ISSN: 2519-6928

Online-ISSN: 3080-7174

Enhancing Heat Transfer Efficiency in a Heat Exchanger Using Green-Synthesized Copper Oxide Nanofluids Based on Ethylene Glycol–Water Mixture

Midya Sabah Rahman[1], Badiea Abdullah Mohammed[1], Hewa Hussein Omar[2]

[1] Department of Chemical Engineering, Faculty of Engineering, Soran University, Kurdistan Region, IRAQ

[2] Department of Petroleum Engineering, Faculty of Engineering, Soran University, Kurdistan Region, IRAQ

DOI: https://doi.org/10.63841/iue3261054

Received 19 Aug 2025; Accepted 29 Sep 2025; Available online 25 Apr 2026.

ABSTRACT:

The efficiency of industrial heat exchangers is limited by the heat transfer coefficient when using traditional fluids. This study introduces a novel sustainable approach for synthesizing copper oxide nanoparticles (CuO NPs), utilizing an eco-friendly route with *Populus Euphratica* leaf extract, a method has never reported before. This work represents the first reported application of green-synthesized CuO nanoparticles in a heat exchanger, marking a novel contribution to sustainable thermal management. The synthesis was optimized at pH of 7, 9, and 11. FTIR, XRD, UV-Vis spectroscopy, and SEM analyses were employed to characterize the CuO NPs to confirm their chemical composition, crystallinity, and morphology. The optimized CuO NPs were dispersed into a different ratio of the base fluid of EG-W at different concentration of CuO NPs ranging from 0.02 % to 0.1 % for enhancing thermal performance. The findings showed that, relative to the base fluid, the overall heat transfer coefficient improved by 40% while the convective heat transfer coefficient in terms of nanofluid increased by about 36 %. The rise in convective heat transfer is attributed not only to the static presence of the nanoparticles but also to Brownian motion and the formation of a liquid nanolayer around the particles. A consistent rise in thermal conductivity as well as the Nusselt number is consistently observed with increasing nanoparticle concentration. These findings confirm the thermal performance benefits of green-synthesized CuO nanofluids and support their potential for industrial heat exchanger applications. Conclusively, the study highlights the viability of green nanotechnology as an environmentally responsible alternative to conventional synthesis for energy-efficient thermal management systems.

Keywords: Green synthesis, CuO nanoparticles, Heat exchanger, Convective heat transfer, Thermal conductivity.

1 INTRODUCTION

Efficient heat transfer is critical in many energy-intensive industries, including power generation, petroleum refining, and chemical processing, where large amounts of heat must be effectively managed to ensure safety, operational reliability, and energy efficiency [1-4]. Conventional heat transfer fluids like water, ethylene glycol, and their mixtures are commonly employed in industrial heat exchangers, because they are widely available and reasonably priced. Their intrinsically low thermal conductivity, which is 0.6 W m^{-1} K^{-1} for water and 0.35 W m^{-1} K^{-1} for 50:50 EG-W at 25ºC, restricts heat transfer performance and frequently leads to larger equipment and higher energy usage [5-7].

Nanofluids, developed by dispersing nanoparticles into conventional base fluids, have attracted widespread interest as a promising approach to overcoming these challenges. Extensive research demonstrates that the addition of metal and metal oxide nanoparticles, including Al_2O_3, TiO_2, ZnO, and CuO, can markedly enhance thermal conductivity, convective heat

1054 *Corresponding author: 501238299005@soran.edu.iq

transfer coefficients, and the overall energy efficiency of heat exchangers [8-11]. Among the different nanoparticle materials, copper oxide has drawn significant interest owing to its relatively high thermal conductivity, excellent chemical stability, cost-effectiveness, and demonstrated efficiency in diverse heat transfer applications [12-15]. For instance, the application of a 0.5 vol% CuO/water nanofluid in combination with single-strip helical screw tape inserts resulted in up to a 32% increase in the Nusselt number, with only a slight increase in the friction factor [16], while 0.2-0.8 vol% in a horizontal ground heat exchanger improved the overall heat transfer rate by 5.3-14.7% [17]. In a shell-and-tube exchanger at 25ºC, 0.05 vol% CuO/water enhanced the convective and overall heat transfer coefficients by 11.39% and 7.08%, respectively [18]. CuO/water–EG (60:40) nanofluid at 0.2 vol% and 70ºC increased thermal conductivity by 36%, enhancing heat transfer performance in an indirect heater [19]. Comparative studies further confirm CuO's advantage over other oxides: at volume fraction equal to 2.5%, CuO/EG achieved 20% higher heat transfer coefficient versus 14% for Al_2O_3/EG [20]; in EG-based systems, 0.06 vol% CuO improved thermal conductivity by 21% compared to 13% for TiO_2, with consistently higher Nusselt numbers [21]; and in water-based systems, CuO outperformed ZnO by up to 12.58% in Nusselt number and 2.61% in thermal performance factor at equal concentration [22]. Furthermore, nanoparticle volume fractions reported in the literature vary widely. For example, some studies have used very low concentrations such as 0.003% [23] or incremental ranges of 0.01%, 0.02%, 0.07%, 0.10%, 0.20%, and 0.40% [24], while others applied narrower intervals of 0.02–0.04–0.06% [21]. Higher loadings have also been examined, including 1.5%, 2%, and 2.5% [25]. This indicates that the nanoparticle concentrations selected in the present work fall within the broad spectrum of values previously explored for CuO-based nanofluids. Despite their advantages, the majority of reported CuO nanoparticle synthesis methods depend on chemical routes that employ hazardous reducing agents or solvents, thereby posing challenges to environmental sustainability and operational safety [26-28]. In recent years, green synthesis methods have gained increasing interest as safer, eco-friendly alternatives for nanoparticle preparation. These approaches utilize plant extracts or other natural agents as reducing and stabilizing agents, eliminating the need for hazardous chemicals while improving nanoparticle stability and dispersion in fluids [29-31]. Reported examples include the use of banana peel extract resulting in particles 60 nm [32], Aloe vera leaf extract yielding particles of 5-20 nm at pH 11.5 [33], Morinda citrifolia leaf extract yielding particles of 20-50 nm at pH 7 [34], and Catha edulis leaf extract resulting in particles 18-28 nm at pH 8 [35]. These studies demonstrate controlled particle size distribution, morphology tuning, and improved stability, which are advantageous for subsequent nanofluid applications. The pH of the synthesis solution is a key parameter influencing the nucleation rate, particle size, and phase purity of CuO nanoparticles [36]. Acidic conditions can lead to incomplete reduction and larger, irregular particles, whereas alkaline pH (9-11) accelerates hydrolysis, producing smaller, highly crystalline, and well-dispersed nanoparticles with improved stability, which is essential for achieving enhanced thermal conductivity and stable nanofluid performance in heat transfer applications [37-39].

However, a critical examination of existing studies reveals two main limitations: (i) very few studies have investigated how synthesis parameters, particularly pH, affect the properties and performance of green-synthesized CuO NPs, despite known evidence that pH strongly influences particle size, crystallinity, and surface characteristics; and (ii) Although the synthesis of CuO NPs using plants has been widely studied, the potential of *Populus Euphratica* leaf extract remains unexplored. Moreover, its integration into nanofluids to enhance the efficiency of heat exchangers represents a unique research direction explored in this study. Unlike prior heat exchanger studies that exclusively employed chemically synthesized CuO, the present study demonstrates, for the first time, the thermal performance of a green-synthesized CuO nanofluid in a shell-and-tube heat exchanger, offering a sustainable and energy-efficient pathway for industrial cooling applications. This work addresses these gaps by introducing a novel, eco-friendly synthesis route for CuO NPs via *Populus Euphratica* extract and by validating their application as a green nanofluid coolant in practical heat exchanger systems.

2 MATERIALS AND METHODS

2.1 MATERIALS

Copper acetate monohydrate [$Cu(CH_3COO)_2 \cdot H_2O$, EMPLURA, ≥98% purity, Merck, Germany], sodium hydroxide (NaOH, pellets, extra pure, assay 97–100.5%, Scharlau, Spain), ethanol (≥99.5% purity, analytical grade, local supplier) and distilled water were purchased and used as received. For nanofluid formulation, reverse osmosis (RO) water and ethylene glycol (EG) (industrial grade, approx. 95–99% purity, local supplier) were used as base fluids. Fresh Populus Euphratica leaves were collected from the Haftaghar–Daqwq region in Iraq and served as the green reducing agent. All experiments were conducted at an ambient laboratory of 23ºC and 40% relative humidity.

2.2 PREPARATION OF PLANT EXTRACT

Fresh *Populus Euphratica* leaves were carefully cleaned to remove surface contaminants and dust, and subsequently dried in the shade at ambient temperature for about two weeks until a constant mass was reached. The dried leaves were finely ground using a high-speed multifunctional comminutor (Model RRH-350A, 28000 rpm). Following the extraction conditions reported in previous green nanoparticle synthesis studies [40, 41], 5 g of the powdered leaves was combined with 100 mL of distilled water in a 250 mL beaker and heated at 70ºC for 1 h under continuous stirring at 500 rpm using a 3G LAB digital magnetic hotplate stirrer. After reaching room temperature, the solution was passed through Whatman

No. 1 filter paper to eliminate residual organic matter, resulting in a clear aqueous extract. The initial pH of the extract was measured between 4 and 5, and the prepared extract was stored at 4ºC until subsequent use in experimental procedures.

2.3 GREEN SYNTHESIS AND CHARACTERIZATION OF CUO NANOPARTICLES

A 0.183 M solution of copper acetate monohydrate was obtained by dissolving 1 g of the salt in 30 mL of distilled water. In a separate step, 25 mL of the filtered plant extract was diluted with 50 mL of distilled water and subsequently introduced dropwise into the copper solution under continuous stirring. As PH is a key factor affecting size, morphology, and stability in plant-mediated nanoparticle synthesis, the pH of the resulting mixture was adjusted to 7, 9, and 11 using 1 M NaOH to study the effect of pH on nanoparticle formation. The resulting mixture was heated at 80 °C for 1 h, during which a gradual color transition from blue to dark brown occurred, confirming the formation of CuO NPs. This transformation is understood to proceed via precipitation of $Cu(OH)_2$, followed by thermal decomposition into CuO, as represented by the following reactions:

$$Cu(CH_3COO)_2.H_2O + 2NaOH + \text{plant Extract (PE)} \rightarrow Cu(OH)_2 + 2CH_3COONa$$

$$Cu(OH)_2 \rightarrow CuO\ (NPs) + H_2O$$

Here, PE refers to the *Populus Euphratica* leaf extract, which contains phytochemicals such as polyphenolic and flavonoid. The –OH and C=O functional groups in these compounds act as reducing agents for Cu^{2+} and as stabilizing ligands to cap and stabilize the nanoparticles, preventing agglomeration during synthesis. The suspension was left overnight to settle and then centrifugation at 8500 rpm for 3 minutes using a laboratory centrifuge (Model H-1600A). The resulting solid was purified by two successive washes with distilled water followed by a single rinse with ethanol, with each washing step subjected to ultrasonication for approximately 1 minute using a Backer vCLEAN ultrasonic cleaner to ensure efficient removal of residual impurities. The washed product was subsequently dried at 80 °C in a LabTech electric drying oven (maximum 250 °C) and calcined at 400 °C for 1 hour in a MFLC-1.6/12 muffle furnace (maximum 1200 ºC) to yield black CuO nano powder. The synthesis procedure is illustrated in Figure 1.

The synthesized CuO nanoparticle were characterized using SEM (Quanta 450, 30 kV, magnification of 20,000x), XRD (2θ range:10°-70°, Cu kα radiation, λ = 1.5406 Å), FTIR (400-4000 cm $^{-1}$), and UV-Vis spectroscopy (200-700 nm) to confirm their structural, chemical, and optical properties.

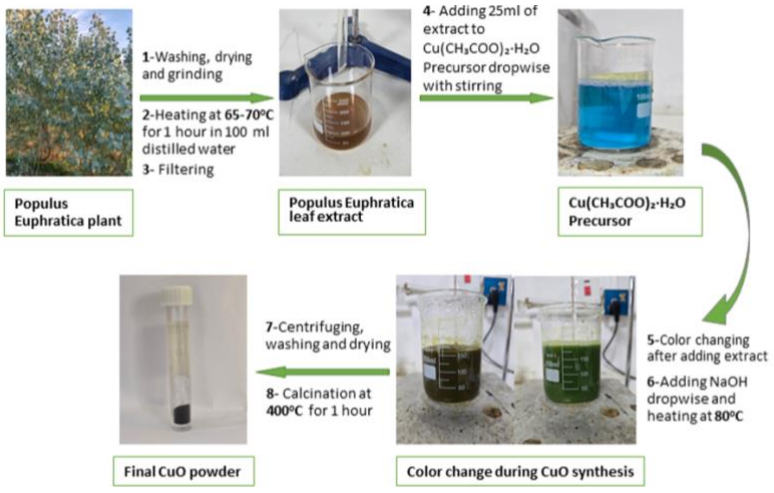

FIGURE 1. Green synthesis route of CuO NPs using *Populus euphratica* leaf extract.

2.4 NANOFLUID PREPARATION

CuO nanofluids were prepared by dispersing the synthesized nanoparticles into a base fluid of RO water and ethylene glycol at different mixing ratio. A total of five nanofluid samples were prepared with CuO NPs volume fraction of 0.02, 0.04, 0.06, 0.08 and 0.1%, which fall within the concentration range frequently reported in earlier CuO nanofluid research. The nanoparticle volume fraction (ϕ) was determined using the following equation:

$$\phi(\%) = \frac{m_p/\rho_p}{m_p/\rho_p + m_{bf}/\rho_{bf}} \times 100 \qquad (1)$$

Where $\emptyset$ is the volume fraction, m_p and m_{bf} represents the masses of CuO NPs and base fluid respectively, and ρ_p and ρ_{bf} denotes their corresponding densities. Each formulation was ultrasonicated using an ultrasonic bath (Model UC-30AL, 6 L tank capacity, 40 kHz frequency) at 25 °C for 1 hour to ensure uniform dispersion and minimize agglomeration. Ultrasonication is widely demonstrated to enhance nanofluid stability and improve nanoparticle distribution. Stability of the prepared nanofluids was monitored by visual sedimentation tests over a period of 3 days, were all samples remained well-dispersed without noticeable settling during this period, indicating sufficient short-term stability for experimental use.

The volume fractions out of the above range were not considered in this study. Concentrations below 0.02% results in negligible thermal performance enhancement, while concentrations above 0.1% led to visible nanoparticle agglomeration and sedimentation, causing unstable flow behavior and unreliable heat transfer measurements during testing.

3 EXPERIMENTAL SETUP

The thermal performance of CuO nanofluids was evaluated using a co-current shell-and-tube heat exchanger equipped with stainless steel tubes measuring 500 mm in length, 0.013 m in inner diameter, and 0.016 m in outer diameter. They were configured in a two-pass flow arrangement with two baffles installed in the shell to enhance fluid mixing and heat transfer. Lubricating oil, which serves as the hot fluid to keep the temperature outside the tube constant, is heated to 90 ºC in a thermostat-controlled insulated bath and then circulated through the exchanger's shell side at 200 L/h flow rate to keep the tube side's thermal boundary stable.

The nanofluid flow rate was initially adjusted to target a Reynolds number of 2000 based on nominal thermophysical properties. However, as the experiment progressed, temperature-dependent changes in viscosity and density caused the actual Reynolds number to vary between 2935 to 3084. This positioned the flow within the transitional regime. Therefore, the Gnielinski correlation was selected for theoretical modeling, as it is valid for $2300 < Re < 5 \times 10^6$ and $0.5 < Pr < 2000$ making it suitable for both transitional and turbulent flow regimes [42-44]. The volume flow rate was varied and monitored using a rotameter calibrated via the volumetric collection method, ensuring an accuracy of ±5%.

Temperature variations were recorded using Four PT-100 resistance temperature detectors type (RTDs) connected to a digital data display which were calibrated against a certified laboratory thermometer at 25°C, 50°C, and 90°C, showing a maximum deviation of 0.2°C (accuracy ≤0.5%). The inlet and outlet temperatures of the nanofluid on the tube side were measured using thermocouples T1 and T2, while T3 and T4 were employed to record the temperatures of the lubricating oil on the shell side.

Flow schematic is presented in Figure 2 and the main thermophysical properties of the working fluids are presented in Table 1. The nanofluids prepared for the experiments had a measured pH of 11, which ensured stable dispersion of the nanoparticles and prevented agglomeration during testing. Six experiments were conducted in total using CuO nanofluids at volume fractions of 0.02, 0.04, 0.06, 0.08, 0.1%. Each test used an 8-litter nanofluid batch and lasted approximately one hour. Thermal steady state was established once the outlet temperatures became stable. Based on the resulting temperature differences, the heat transfer coefficient was calculated to assess the cooling efficiency of the nanofluid. To further ensure reliability, selected runs were repeated under identical conditions, and the results showed close agreement. The reported values represent averages of steady-state measurements, thereby minimizing random fluctuations and enhancing reproducibility of the data.

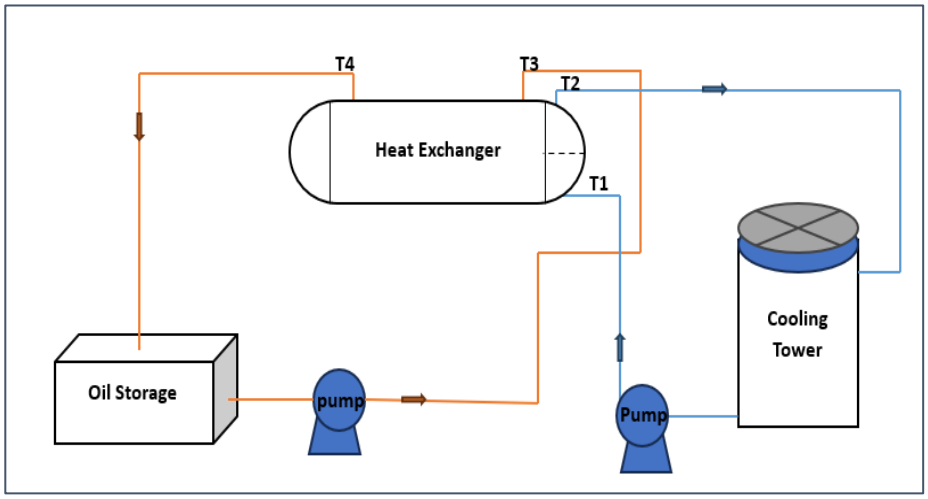

FIGURE 2. Schematic flow diagram showing the working fluid paths and sensor layout (T1–T4).

Table 1. Physicochemical properties of the working fluids used in this study: heavy lubricating oil (ASIA Co., Tanjero – Sulaymaniyah, Iraq), reverse osmosis (RO) water (Fers Co., Arbet – Sulaymaniyah, Iraq) and ethylene glycol (Gagro Co., Erbil, Iraq).

Property	Heavy Lubricating Oil	Reverse Osmosis (RO)Water	Ethylene Glycol
Viscosity	28 cp (at 50°C)	0.88	16.04 cp
Density / Specific Gravity	0.887 (Sp.Gr.at 15.6°C)	0.997	1.114 g/cm^3
Boiling Point °C	_	100	197.3°C
Freezing point / Pour Point (°C)	-6°C (Pour Point)	0	-11.2°C (Freezing Point)
Flash Point (°C)	204°C	_	_
pH	_	6.5	_
Electrical Conductivity	_	48 µS	1.07 × 10^{-6} mhos/cm (at 20°C)
TDS (ppm)	_	24 ppm	_
NaCl (%)	_	0.1 %	_
Thermal Conductivity (W/m.K)	0.13	0.613	0.252
Specific Heat Capaciy (J/kg.K)	2100	4180	2415

4 GOVERNING THERMAL-HYDRAULIC EQUATIONS

To assess the thermal behavior of CuO–EG/W nanofluids within the shell-and-tube heat exchanger, standard heat transfer and fluid flow relations were applied to determine the Reynolds number, Prandtl number, thermal conductivity, convective heat transfer coefficient and Nusselt number.

The Reynolds number (Re) can be calculated to characterize the flow regime [45]:

$$Re = \frac{\rho_{nf}\, d_i\, v}{\mu_{nf}} \tag{2}$$

where ρ_{nf} denotes the nanofluid density (kg/m³), d_i represents the inner diameter of the tube (m), $\boldsymbol{v}$ corresponds to the nanofluid velocity (m/s), and μ_{nf} indicates the nanofluid viscosity (Pa·s).

The Prandtl number (Pr) was calculated as [46]:

$$\mathrm{Pr} = \frac{\mu\ c_p}{k} \tag{3}$$

c_p denotes the specific heat capacity (J/kg·K), μ represents the dynamic viscosity (pa.s), and k corresponds thermal conductivity (W/m·K) of the nanofluid.

The thermal conductivity of the nanofluid was estimated using the Maxwell model [47]:

$$k_{nf} = k_{bf} \cdot \frac{k_p + 2k_{bf} + 2\phi(k_p - k_{bf})}{k_p + 2k_{bf} - \phi(k_p - k_{bf})} \tag{4}$$

where k_{nf}, k_{bf} and k_p represent the thermal conductivities of the nanofluid, base fluid, and nanoparticle respectively, and ϕ denotes the nanoparticle volume fraction.

The heat transfer rate was computed on both the hot and cold sides using [48]:

$$Q_h = m_h\ c_{ph}\ (T_{hi} - T_{ho}) \tag{5}$$

$$Q_c = m_c\ c_{pc}\ (T_{co} - T_{ci}) \tag{6}$$

and the average heat transfer rate was [49]:

$$Q_{avg} = \frac{Q_h + Q_c}{2} \tag{7}$$

Where Q_h denotes the heat lost by the hot fluid and Q_c denotes the heat gained by the cold fluid.

The experimental convective heat transfer coefficient was then obtained as [50]:

$$h_i = \frac{Q_{avg}}{A_i(T_w - T_b)} \tag{8}$$

where A is the internal surface area of the tube, T_w is the wall temperature (assumed equal to shell-side temperature), and T_b is the bulk temperature of the nanofluid.

The Nusselt number (Nu), indicating the enhancement of convective heat transfer, was calculated using [51]:

$$Nu = \frac{h \cdot d_i}{k_{nf}} \tag{9}$$

The theoretical Nusselt number was predicted using the Gnielinski correlation [52]:

$$Nu = \frac{(f/8)(Re - 1000)Pr}{1 + 12.7\sqrt{(f/8)}\,(\mathrm{Pr}^{\frac{2}{3}} - 1)} \tag{10}$$

with the friction factor f given by [53]:

$$f = (0.79\,.\,ln\,Re - 1.64\,)^{-2} \tag{11}$$

5 RESULTS AND DISCUSSION

5.1 FTIR ANALYSIS

FTIR analysis was carried out to examine the functional groups associated with CuO NPs formation at different pH values, with the resulting spectra at pH 7, 9, and 11 illustrated in Figure 3. Strong absorption bands in the 400–650 cm^{-1} range were seen in all samples, which were ascribed to CuO stretching vibrations and verified that copper oxide had successfully formed. These bands are in good agreement with the previously studied FTIR spectra of CuO,[54] confirming the correct assignment. O-H stretching is represented by a broad band at about 3400 cm^{-1}, most likely as a result of adsorbed water or hydroxyl groups. Peaks near 1600 cm^{-1} are associated with H-O-H bending or organic residues from the plant extract. The spectrum at pH 11 showed more defined CuO peaks, indicating enhanced crystallinity and fewer residual impurities under alkaline conditions. The enhanced spectral definition at pH 11 is consistent with the XRD results (Section 5.2), which confirmed higher crystallinity, and with the SEM observations (Section 5.4) showing better-defined particle morphology. Together, these results validate those alkaline conditions facilitate the synthesis of purer and more crystalline CuO NPs using *Populus euphratica* extract.

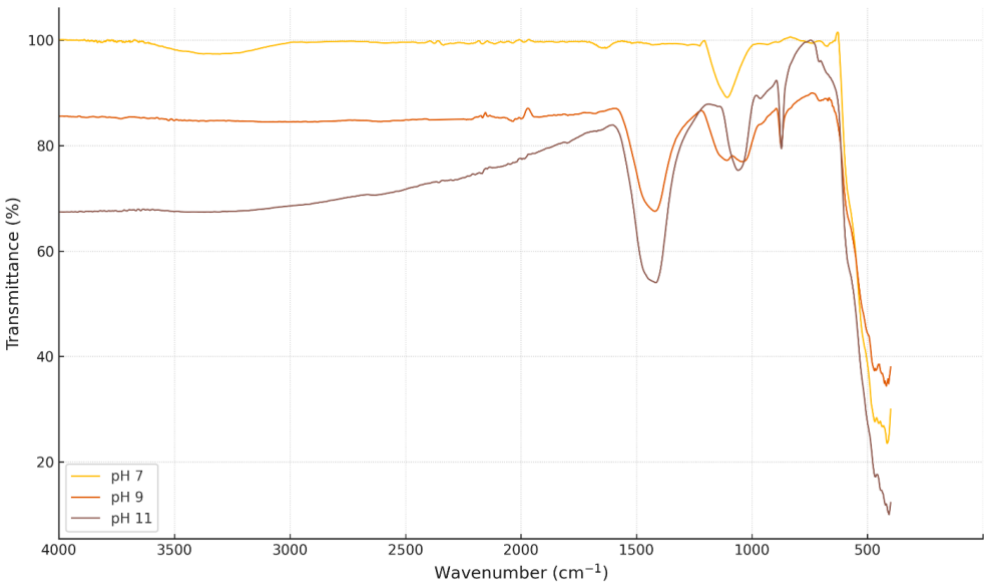

FIGURE 3. FTIR spectra of CuO nanoparticles synthesized at pH 7, 9, and 11.

5.2 XRD ANALYSIS

The phase structure and crystallinity of CuO NPs prepared at pH values of 7, 9 and 11 were examined using X-ray diffraction (XRD), as shown in Figure 4. Distinct diffraction peaks were recorded for all samples, corresponding to monoclinic CuO. The major peaks appeared around 2θ = 32.5°, 35.5°, 38.7°, 48.7°, 53.4°, 58.3°, and 61.5°, which matched the lattice planes (110), (-111), (111), (-202), (020), (202), and (-113) of monoclinic CuO. These results are in agreement with the JCPDS card No. 48-1548. The absence of additional peaks indicated that the obtained nanoparticles were phase-pure CuO.

Notably, the CuO NPs synthesized at pH 11 exhibited the sharpest and most intense peaks, indicating improved crystallinity and better-ordered crystalline domains, which is consistent with previous reports that higher synthesis pH leads to sharper XRD peaks, reduced FWHM, and enhanced crystallinity in CuO NPs [55-57]. In contrast, broader peaks at lower pH values suggest less crystalline and potentially larger or more irregular nanoparticles. This trend supports the understanding that increasing the pH during green synthesis favors enhanced nucleation and crystal growth kinetics, ultimately leading to finer, more uniform CuO NPs with higher phase purity [58].

The crystallite size of the CuO NPs was estimated using the Debye–Scherrer equation:

$$D = \frac{K\lambda}{\beta \cos\theta} \tag{12}$$

where K is the shape factor (0.9), λ is the X-ray wavelength (0.15406 nm for Cu Kα), β is the full width at half maximum (FWHM) of the diffraction peak in radians, and θ is the Bragg angle. The calculated crystallite sizes were 26, 29, and 42 nm for pH 7, 9, and 11, respectively, indicating enhanced crystal growth at higher alkalinity, which is beneficial for improving thermal conductivity and thus supports the superior heat transfer performance of the pH 11 nanofluid

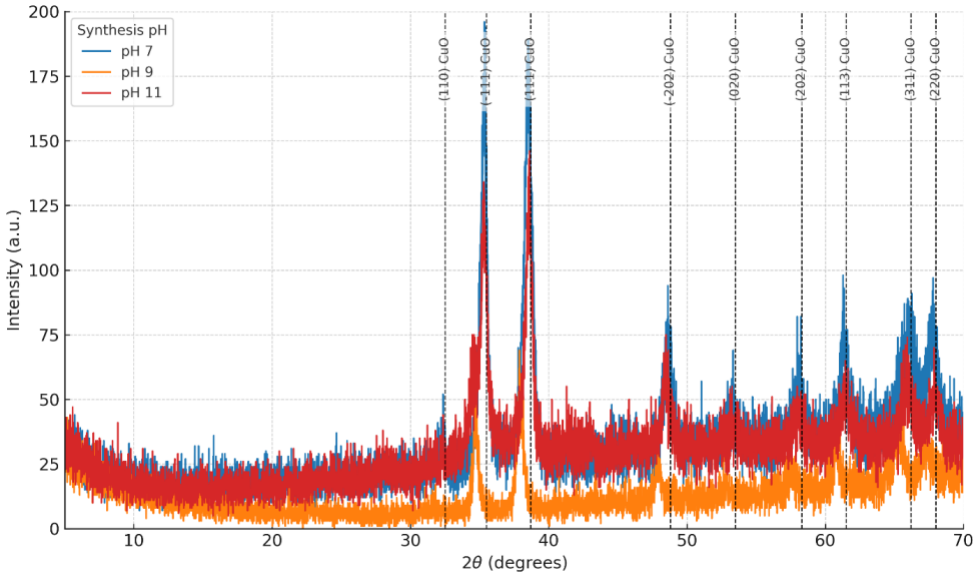

FIGURE 4. X-ray diffraction spectra of CuO NPs synthesized at pH 7, 9, and 11, showing characteristic peaks of monoclinic CuO (JCPDS 48-1548).

5.3 UV–VIS SPECTROSCOPY

The UV-Vis absorption spectra of CuO NPs synthesized under pH conditions of 7, 9 and 11 are shown in Figure 5. All samples exhibited broad absorption features in the UV region (200–400 nm), characteristic of nanoscale CuO. The highest absorbance intensity was observed for the pH 11 sample, likely due to a greater nanoparticle population or enhanced dispersion. A clear redshift in the absorption edge was noted with increasing pH, and the estimated optical band gaps were approximately 3.25 eV (pH 7), 1.76 eV (pH 9), and 1.44 eV (pH 11).

The observed band gap reduction is typically associated with increased particle size or crystallinity. However, this trend may also reflect fewer surface states and improved electronic coupling under alkaline synthesis conditions. While XRD indicates smaller crystallite domains at higher pH, UV-Vis measurements are also sensitive to morphology, surface defects, and interparticle interactions. Thus, the combined data suggest that pH 11 promotes structurally ordered, optically active nanoparticles with reduced quantum confinement and fewer defects.

5.4 SCANNING ELECTRON MICROSCOPY (SEM)

SEM analysis was employed to study the surface morphology of CuO NPs formed at pH 7, 9 and 11, with the resulting micrographs presented in Figure 6. All samples display agglomerated yet distinct nanoparticles, confirming successful nanoscale formation. At pH 7, the particles appear highly aggregated with poor individual definition. In contrast, the pH 9 sample reveals moderately dispersed grains with emerging uniformity. Notably, the pH 11 sample exhibits more clearly defined, relatively uniform spherical-like nanoparticles, indicating enhanced growth control and reduced agglomeration under alkaline conditions.

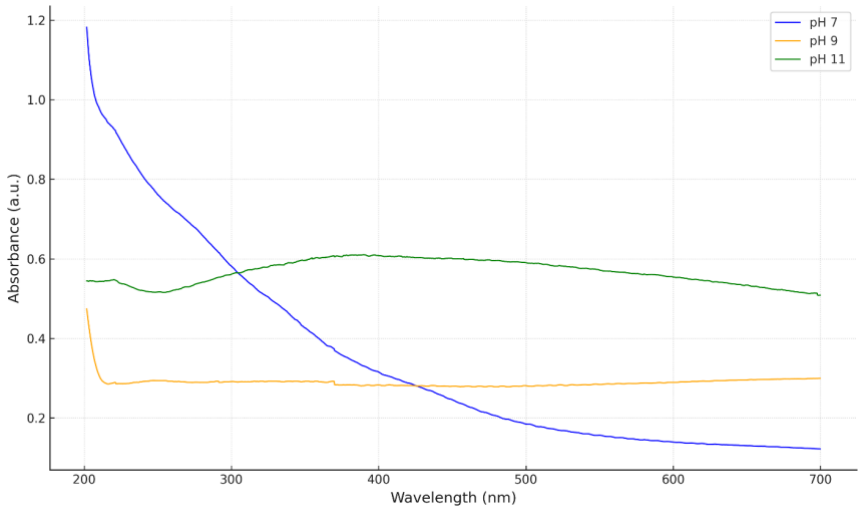

FIGURE 5. UV-Vis absorbance spectra of CuO NPs at pH 7, 9, and 11.

The improved morphological regularity at higher pH may be attributed to increased nucleation rates and better electrostatic stabilization in basic media, which promote more uniform particle growth. While SEM does not measure crystallite size directly, the apparent increase in particle definition and shape consistency complements XRD results indicating higher crystallinity. These morphological features especially at pH 11 are favorable for heat transfer and dispersion in nanofluid systems due to their likely impact on stability and surface area-to-volume ratio. The average particle sizes derived from SEM analysis were 27.5 ± 18.3 nm, 37.6 ± 15 nm, and 35.6 ± 22.2 nm for pH 7, 9, and 11, respectively, as shown in the particle size distribution histograms Figure 7. More uniformly defined nanoparticles at pH 11 indicate reduced agglomeration tendency under alkaline conditions, which is favorable for stable nanofluid formation. These morphological characteristics correlate with the superior thermal performance observed for the pH 11 nanofluid.

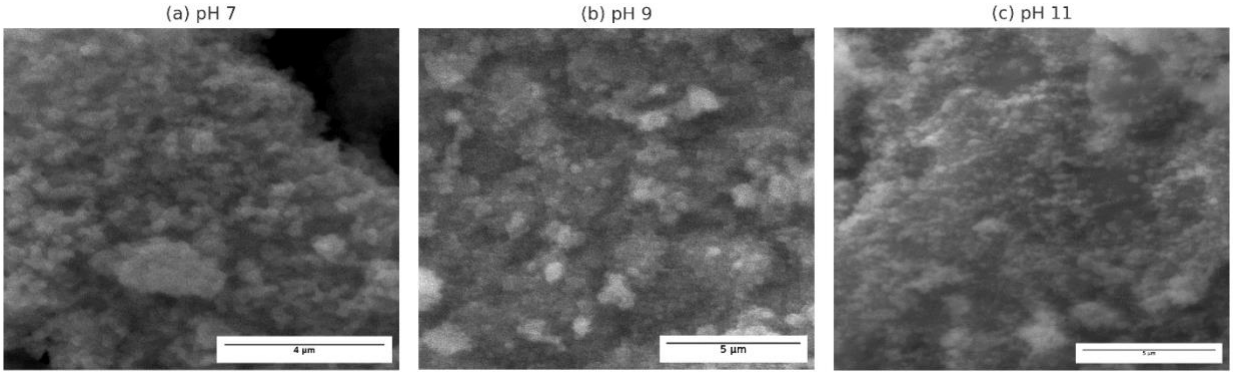

FIGURE 6. SEM images of CuO NPs synthesized at pH 7, 9, and 11.

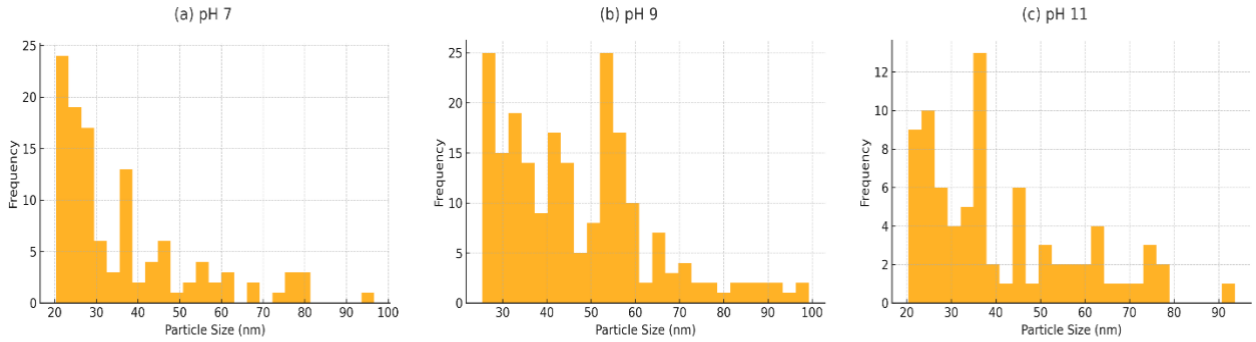

FIGURE 7. Particle size distributions of CuO NPs synthesized at (a) pH 7, (b) pH 9, and (c) pH 11 based on SEM analysis.

5.5 THERMAL PERFORMANCE EVALUATION

As illustrated in Figure 8, the CuO–EG/water nanofluids exhibited a marked rise in the convective heat transfer coefficient as the nanoparticle concentration increased. The experimental results show a steady rise in heat transfer coefficient from 745.98 W/m²·K to 1011.21 W/m²·K, corresponding to an improvement of 36% compared with the base fluid. Beyond the concentration range of 0.02–0.10 vol%, however, the enhancement was negligible (data not shown). The observed improvement is attributed to higher effective thermal conductivity, intensified micro-convection induced by Brownian motion, enhanced thermal interaction between the nanofluid and tube surfaces, and the relatively low flow resistance of the nanofluids.

Theoretical predictions based on the Gnielinski correlation exhibit a similar upward trend, with values ranging from 778.77 to 1048.67 W/m²·K. Although experimental results remain slightly below the theoretical prediction over the tested range. The overall agreement supports the applicability of the Gnielinski correlation for predicting convective heat transfer in transition nanofluid flows. An observed gap also highlights the role of real-world factors such as nanoparticle aggregation, thermal resistance, or imperfect dispersion, which may reduce actual heat transfer efficiency compared to idealized theoretical assumptions. In addition, the experiments were conducted fully in the transitional regime (Re = 2935–3084). Although the Gnielinski correlation has been extended to this range, its accuracy is strongest in the fully turbulent region, and flow near the lower boundary (Re < 3000) remains unstable and difficult to model. This regime-related limitation likely contributes to the observed discrepancy between experimental and predicted values. When compared with previous reports on CuO nanofluids, the present green-synthesized system demonstrates competitive performance. A CuO/EG–water (60:40) nanofluid achieved up to 67% enhancement at 0.06 vol% under fully turbulent flow conditions [59], while another study on CuO/EG–water (80:20) reported 40-45% improvement at 0.2 vol% [60]. Similarly, CuO/EG–water (75:25) applied in a PV/T cooling system yielded 39.6% thermal efficiency enhancement at 2.0 wt% [61]. These values confirm that the enhancement achieved in the present work lies within the range of chemically synthesized systems, despite being obtained at lower nanoparticle loading, with a more dilute EG–water base fluid, and under transitional flow conditions. The favorable crystallinity and dispersion stability of the green-synthesized CuO NPs likely contributed to this competitive performance. The differences in thermal performance reported in other studies may arise from variations in chemically synthesis method, base fluid composition, or operating conditions all of which can significantly influence overall efficiency.

Figure 9 shows that the Nusselt number (*Nu*) values are significantly greater than 1, confirming that heat transfer is dominated by convection. A clear upward trend in Nu with increasing CuO NPs concentration demonstrates more efficient convective transport from the fluid to the tube wall, reflected in the strengthened thermal interaction at the fluid–solid interface and consistent with the rise in the convective heat transfer coefficient. According to the Gnielinski correlation, the calculated *Nu* follows a similar upward trend, with slight overestimation at higher concentrations. Despite this minor deviation, the consistent alignment between experimental and theoretical results confirms the applicability of the Gnielinski model in estimating the heat transfer behavior of nanofluids in transitional flow regimes. The observed *Nu* enhancement also highlights the role of nanoparticles in disturbing the boundary layer and intensifying micro-convection. Additionally, the overall heat transfer coefficient exhibited an increase of approximately 40% relative to the base fluid, further reinforcing the enhanced thermal performance observed across all indicators. To further interpret these enhancements and the underlying boundary layer behavior, the Prandtl number (*Pr*) was evaluated as a complementary parameter.

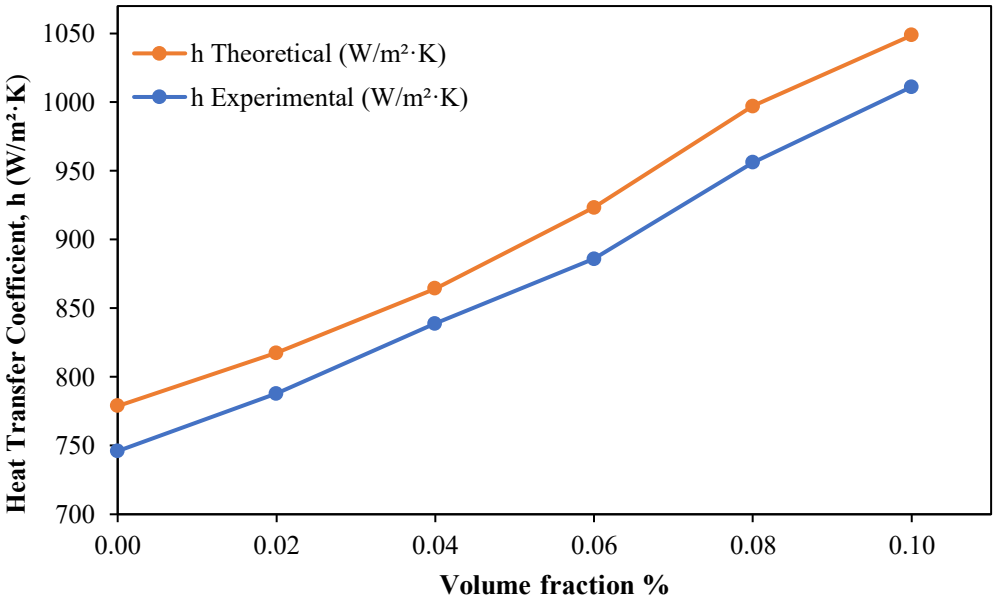

FIGURE 8. Experimental and predicted convective heat transfer coefficients of CuO–EG/water (20:80) nanofluid at varying nanoparticle volume fractions.

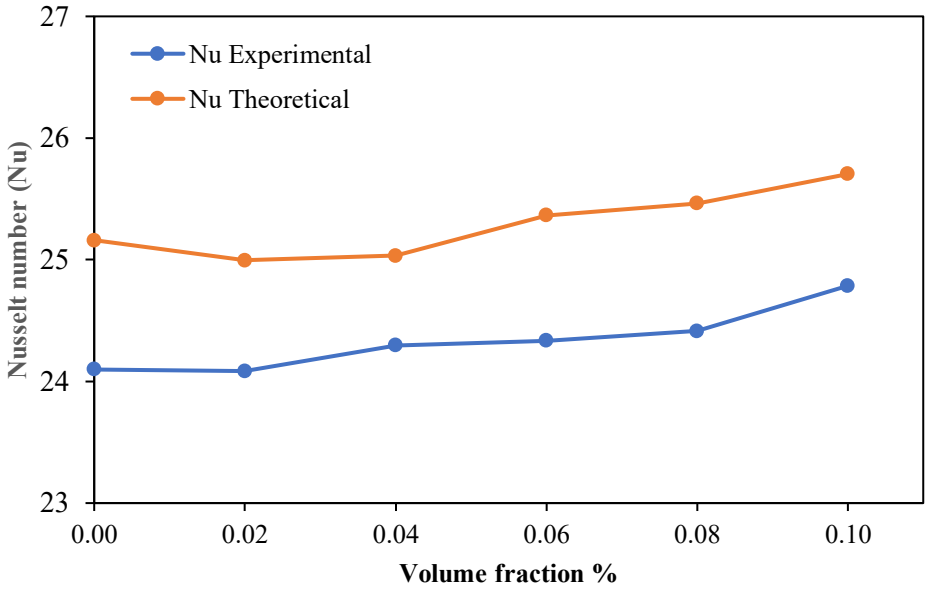

FIGURE 9. Nusselt number of CuO–EG: Water nanofluid at different nanoparticle volume concentrations, comparing experimental data with theoretical predictions.

As shown in Figure 10, the Prandtl number in this study ranged from 10.61 at 0 % volume fraction to 9.36 at 0.1 %, remaining well above 1 and confirming that momentum diffusivity is significantly greater than thermal diffusivity. This condition leads to the development of a thermal boundary layer that is comparatively thinner than the velocity boundary layer, resulting in a large temperature gradient near the tube wall and enhancing convective heat transfer. The gradual decrease in *Pr* with increasing CuO concentration is attributed to the enhancement in thermal conductivity surpassing the modest increase in dynamic viscosity. This shift means heat diffuses relatively faster at higher nanoparticle loadings, while the consistently high *Pr* values preserve the favorable boundary layer structure that supports the observed increases in Nusselt number and heat transfer coefficient [1, 62-64].

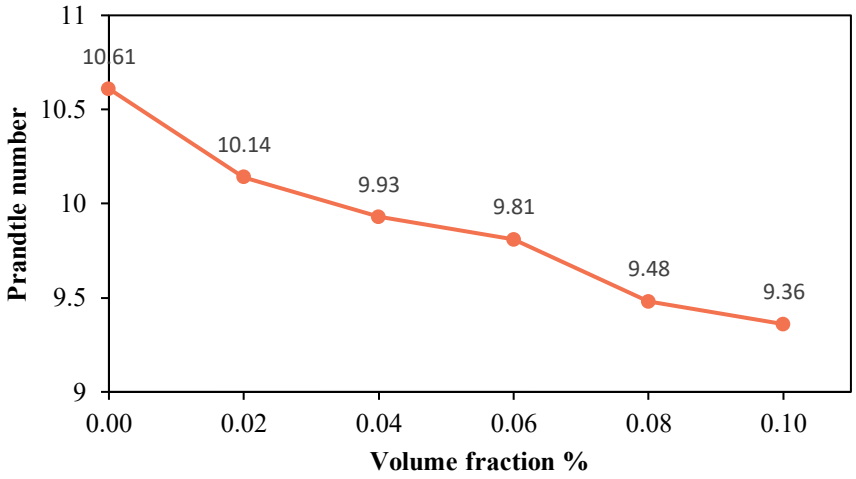

FIGURE 10. Decreasing Prandtl number with increasing nanoparticle volume fraction for CuO–water/EG nanofluid.

Figure 11 illustrates that the prediction of Maxwell's model shows an increase in the nanofluids thermal conductivity ratio k_{nf}/k_{bf}, where $k_{nf}$and k_{bf} represent the thermal conductivities of the nanofluid and base fluid, respectively, from 1.056 to 1.318 over the tested concentration. This enhancement is results from the high intrinsic conductivity of CuO, the formation of conductive pathways within the fluid, and intensified nanoparticle Brownian motion, all of which improve microscopic thermal energy transport [1, 65].

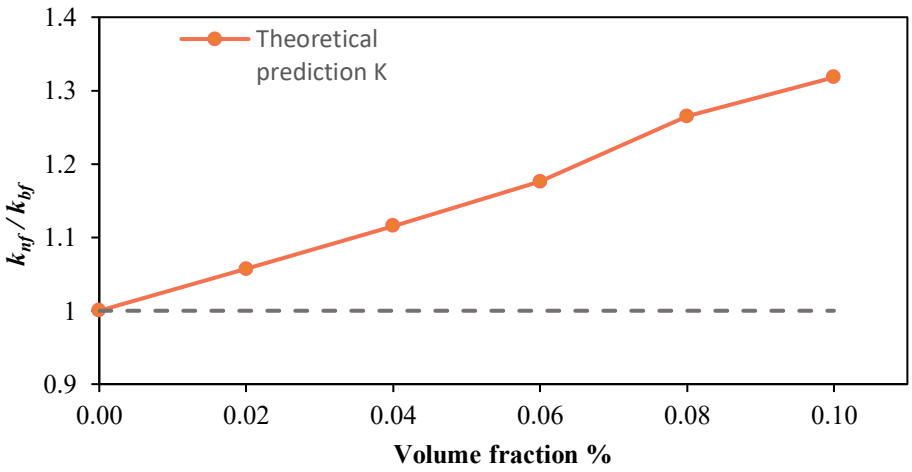

FIGURE 11. Predicted enhancement ratio of thermal conductivity k_{nf}/k_{bf} for CuO EG: Water (20:80) nanofluid calculated using the Maxwell model at different nanoparticle volume fractions. The dashed line indicates the base fluid level (k_{nf}/k_{bf} = 1.0).

CONCLUSION

In this study, copper oxide nanoparticles were successfully synthesized via an innovative green approach utilizing *Populus Euphratica* leaf extract. This specific plant extract has not been previously reported for CuO synthesis, marking a significant novel contribution to sustainable thermal management research. The synthesis was meticulously optimized at pH levels of 7, 9, and 11 to ensure desired nanoparticle properties. Characterization via FTIR, XRD, UV-Vis spectroscopy, and SEM confirmed the nanoparticles' chemical composition, crystallinity, and morphology. Dispersing the optimized CuO nanoparticles into an ethylene glycol–water (EG–W) base fluid consistently yielded significant improvements in thermal performance. Relative to the base fluid, the convective heat transfer coefficient increased by

~36%, and the overall heat transfer coefficient by nearly 40%. In addition, both the thermal conductivity and Nusselt number of the nanofluid demonstrated measurable gains, confirming the beneficial influence of CuO NPs incorporation.

These enhancements are attributed to a combination of factors:

- Improved effective thermal conductivity of the nanofluid.
- Intensified micro-convection due to nanoparticle movement (e.g., Brownian motion).
- Achieved stable nanoparticle dispersion within the base fluid, facilitated by the green synthesis method.

Overall, these findings strongly confirm the significant potential of green-synthesized nanomaterials for enhancing heat exchanger performance. This approach not only offers an effective solution for improved thermal management but also promotes eco-friendly, sustainable synthesis methods by eliminating reliance on hazardous chemicals often used in conventional nanoparticle production. Upcoming research should emphasize dispersion stability over extended periods, the practicality of industrial-scale synthesis, and performance under broader operating conditions.

FUNDING

No funding was received for conducting this study.

ACKNOWLEDGEMENT

The authors would like to express their gratitude to the head of the chemical engineering at Soran university in

Iraq for providing laboratory facilities.

CONFLICTS OF INTEREST

The author declares no conflict of interest.

DATA AVAILABILITY

The data underlying this article will be shared on reasonable request to the corresponding author.

REFERENCES

[1] P. Keblinski, J. A. Eastman, and D. G. Cahill, "Nanofluids for thermal transport," Materials Today, vol. 8, no. 6, pp. 36-44, 2005/06/01/ 2005, doi: https://doi.org/10.1016/S1369-7021(05)70936-6.

[2] R. Saidur, K. Y. Leong, and H. A. Mohammed, "A review on applications and challenges of nanofluids," Renewable and Sustainable Energy Reviews, vol. 15, no. 3, pp. 1646-1668, 2011/04/01/ 2011, doi: https://doi.org/10.1016/j.rser.2010.11.035.

[3] F. Friedler, "Process integration, modelling and optimisation for energy saving and pollution reduction," Applied Thermal Engineering, vol. 30, no. 16, pp. 2270-2280, 2010/11/01/ 2010, doi: https://doi.org/10.1016/j.applthermaleng.2010.04.030.

[4] A. Patel, "Heat Exchangers in Industrial Applications: Efficiency and Optimization Strategies," International Journal of Engineering Research and, vol. 12, 09/28 2023, doi: 10.17577/IJERTV12IS090003.

[5] E. T. Bello et al., "Nano-coolants for thermal enhancement in heat exchangers: A review of prospects, challenges and applications," Next Nanotechnology, vol. 8, p. 100214, 2025/01/01/ 2025, doi: https://doi.org/10.1016/j.nxnano.2025.100214.

[6] L. S. Sundar, M. K. Singh, and A. C. M. Sousa, "Enhanced heat transfer and friction factor of MWCNT–Fe3O4/water hybrid nanofluids," International Communications in Heat and Mass Transfer, vol. 52, pp. 73-83, 2014/03/01/ 2014, doi: https://doi.org/10.1016/j.icheatmasstransfer.2014.01.012.

[7] P. Zhang, X. Jiang, P. Yuan, H. Yan, and D. Yang, "Silver nanopaste: Synthesis, reinforcements and application," International Journal of Heat and Mass Transfer, vol. 127, pp. 1048-1069, 2018/12/01/ 2018, doi: https://doi.org/10.1016/j.ijheatmasstransfer.2018.06.083.

[8] S. U. Choi and J. A. Eastman, "Enhancing thermal conductivity of fluids with nanoparticles," Argonne National Lab.(ANL), Argonne, IL (United States), 1995.

[9] V. Ghazanfari, A. Taheri, Y. Amini, and F. Mansourzade, "Enhancing heat transfer in a heat exchanger: CFD study of twisted tube and nanofluid (Al2O3, Cu, CuO, and TiO2) effects," Case Studies in Thermal Engineering, vol. 53, p. 103864, 2024/01/01/ 2024, doi: https://doi.org/10.1016/j.csite.2023.103864.

[10] W. Ajeeb, R. R. S. Thieleke da Silva, and S. M. S. Murshed, "Experimental investigation of heat transfer performance of Al2O3 nanofluids in a compact plate heat exchanger," Applied Thermal Engineering, vol. 218, p. 119321, 2023/01/05/ 2023, doi: https://doi.org/10.1016/j.applthermaleng.2022.119321.

[11] A. H. Rasheed, H. Alias, and S. D. Salman, "Thermophysical Properties for ZnO-Water Nanofluid: Experimental Study," Materials Science Forum, vol. 1025, pp. 9-14, 2021, doi: 10.4028/www.scientific.net/MSF.1025.9.

[12] R. Agarwal, K. Verma, N. K. Agrawal, R. K. Duchaniya, and R. Singh, "Synthesis, characterization, thermal conductivity and sensitivity of CuO nanofluids," Applied Thermal Engineering, vol. 102, pp. 1024-1036, 2016.

[13] D. K. Devendiran and V. A. Amirtham, "A review on preparation, characterization, properties and applications of nanofluids," Renewable and Sustainable Energy Reviews, vol. 60, pp. 21-40, 2016.

[14] A. S. Tijani and A. S. b. Sudirman, "Thermos-physical properties and heat transfer characteristics of water/anti-freezing and Al2O3/CuO based nanofluid as a coolant for car radiator," International Journal of Heat and Mass Transfer, vol. 118, pp. 48-57, 2018/03/01/ 2018, doi: https://doi.org/10.1016/j.ijheatmasstransfer.2017.10.083.

[15] W. Sun, T. Xiao, Q. Liu, J. Zhao, and C. Liu, "Experimental study on glycerol/aldehyde or ketone binary nanofluids for thermal management," International Journal of Heat and Mass Transfer, vol. 214, p. 124463, 2023/11/01/ 2023, doi: https://doi.org/10.1016/j.ijheatmasstransfer.2023.124463.

[16] S. R. Chaurasia and R. M. Sarviya, "Thermal performance analysis of CuO/water nanofluid flow in a pipe with single and double strip helical screw tape," Applied Thermal Engineering, vol. 166, p. 114631, 2020/02/05/ 2020, doi: https://doi.org/10.1016/j.applthermaleng.2019.114631.

[17] R. Du, D. Jiang, Y. Wang, and S. Kwok Wei, "An experimental investigation of CuO/water nanofluid heat transfer in geothermal heat exchanger," Energy and Buildings, vol. 227, p. 110402, 08/01 2020, doi: 10.1016/j.enbuild.2020.110402.

[18] Z. Said, S. M. A. Rahman, M. El Haj Assad, and A. H. Alami, "Heat transfer enhancement and life cycle analysis of a Shell-and-Tube Heat Exchanger using stable CuO/water nanofluid," Sustainable Energy Technologies and Assessments, vol. 31, pp. 306-317, 2019/02/01/ 2019, doi: https://doi.org/10.1016/j.seta.2018.12.020.

[19] A. R. Rahmati and M. Reiszadeh, "Experimental study on the effect of copper oxide nanoparticles on thermophysical properties of ethylene glycol–water for using in indirect heater at city gate stations," Journal of Thermal Analysis and Calorimetry, vol. 135, no. 1, pp. 73-82, 2019/01/01 2019, doi: 10.1007/s10973-017-6946-4.

[20] A. Zamzamian, S. N. Oskouie, A. Doosthoseini, A. Joneidi, and M. Pazouki, "Experimental investigation of forced convective heat transfer coefficient in nanofluids of Al2O3/EG and CuO/EG in a double pipe and plate heat exchangers under turbulent flow," Experimental Thermal and Fluid Science, vol. 35, no. 3, pp. 495-502, 2011/04/01/ 2011, doi: https://doi.org/10.1016/j.expthermflusci.2010.11.013.

[21] N. Kumar and S. S. Sonawane, "Experimental study of thermal conductivity and convective heat transfer enhancement using CuO and TiO2 nanoparticles," International Communications in Heat and Mass Transfer, vol. 76, pp. 98-107, 2016/08/01/ 2016, doi: https://doi.org/10.1016/j.icheatmasstransfer.2016.04.028.

[22] B. K. Ahirwar and A. Kumar, "Comparative analysis of CuO–water and ZnO–water nanofluids in the turbulent regime for enhanced performance in double-pipe heat exchanger," Journal of Thermal Analysis and Calorimetry, vol. 149, no. 23, pp. 14213-14240, 2024/12/01 2024, doi: 10.1007/s10973-024-13623-5.

[23] L. G. Asirvatham, N. Vishal, S. K. Gangatharan, and D. M. Lal, "Experimental Study on Forced Convective Heat Transfer with Low Volume Fraction of CuO/Water Nanofluid," Energies, vol. 2, no. 1, pp. 97-119doi: 10.3390/en20100097.

[24] M.-H. Chang, H.-S. Liu, and C. Y. Tai, "Preparation of copper oxide nanoparticles and its application in nanofluid," Powder Technology, vol. 207, no. 1, pp. 378-386, 2011/02/15/ 2011, doi: https://doi.org/10.1016/j.powtec.2010.11.022.

[25] S. Z. Heris, F. Mohammadpur, O. Mahian, and A. Z. Sahin, "Experimental Study of Two Phase Closed Thermosyphon Using Cuo/Water Nanofluid in the Presence Of Electric Field," Experimental Heat Transfer, vol. 28, no. 4, pp. 328-343, 2015/07/04 2015, doi: 10.1080/08916152.2014.883448.

[26] S. Iravani, H. Korbekandi, S. V. Mirmohammadi, and B. Zolfaghari, "Synthesis of silver nanoparticles: chemical, physical and biological methods," Research in pharmaceutical sciences, vol. 9, no. 6, pp. 385-406, 2014.

[27] S. A. Nada, R. M. El-Zoheiry, M. Elsharnoby, and O. S. Osman, "Enhancing the thermal performance of different flow configuration minichannel heat sink using Al2O3 and CuO-water nanofluids for electronic cooling: An

experimental assessment," International Journal of Thermal Sciences, vol. 181, p. 107767, 2022/11/01/ 2022, doi: https://doi.org/10.1016/j.ijthermalsci.2022.107767.

[28] M. Khooshechin, S. Fathi, F. Salimi, and S. Ovaysi, "The influence of surfactant and ultrasonic processing on improvement of stability and heat transfer coefficient of CuO nanoparticles in the pool boiling," International Journal of Heat and Mass Transfer, vol. 154, p. 119783, 2020/06/01/ 2020, doi: https://doi.org/10.1016/j.ijheatmasstransfer.2020.119783.

[29] R. A. Banjara, A. Kumar, R. K. Aneshwari, M. L. Satnami, and S. K. Sinha, "A comparative analysis of chemical vs green synthesis of nanoparticles and their various applications," Environmental Nanotechnology, Monitoring & Management, vol. 22, p. 100988, 2024/12/01/ 2024, doi: https://doi.org/10.1016/j.enmm.2024.100988.

[30] A. Ullah and S. I. Lim, "Plant extract-based synthesis of metallic nanomaterials, their applications, and safety concerns," Biotechnology and Bioengineering, vol. 119, no. 9, pp. 2273-2304, 2022.

[31] S. Ahmed, M. Ahmad, B. L. Swami, and S. Ikram, "A review on plants extract mediated synthesis of silver nanoparticles for antimicrobial applications: a green expertise," Journal of advanced research, vol. 7, no. 1, pp. 17-28, 2016.

[32] M. Aminuzzaman, L. M. Kei, and W. H. Liang, "Green synthesis of copper oxide (CuO) nanoparticles using banana peel extract and their photocatalytic activities," AIP Conference Proceedings, vol. 1828, no. 1, 2017, doi: 10.1063/1.4979387.

[33] S. Sharma and K. Kumar, "Aloe-vera leaf extract as a green agent for the synthesis of CuO nanoparticles inactivating bacterial pathogens and dye," Journal of Dispersion Science and Technology, vol. 42, no. 13, pp. 1950-1962, 2021/11/02 2021, doi: 10.1080/01932691.2020.1791719.

[34] M. Priya et al., "Green synthesis, characterization, antibacterial, and antifungal activity of copper oxide nanoparticles derived from Morinda citrifolia leaf extract," Scientific Reports, vol. 13, no. 1, p. 18838, 2023/11/01 2023, doi: 10.1038/s41598-023-46002-5.

[35] W. W. Andualem, F. K. Sabir, E. T. Mohammed, H. H. Belay, and B. A. Gonfa, "Synthesis of Copper Oxide Nanoparticles Using Plant Leaf Extract of Catha edulis and Its Antibacterial Activity," Journal of Nanotechnology, vol. 2020, no. 1, p. 2932434, 2020/01/01 2020, doi: https://doi.org/10.1155/2020/2932434.

[36] M. Shahmiri et al., "Effect of pH on the Synthesis of CuO Nanosheets by Quick Precipitation Method," WSEAS Transactions on Environment and Development, 04/01 2013.

[37] K. Phiwdang, S. Suphankij, W. Mekprasart, and W. Pecharapa, "Synthesis of CuO Nanoparticles by Precipitation Method Using Different Precursors," Energy Procedia, vol. 34, pp. 740-745, 2013/01/01/ 2013, doi: https://doi.org/10.1016/j.egypro.2013.06.808.

[38] R. Manimaran, K. Palaniradja, N. Alagumurthi, S. Sendhilnathan, and J. Hussain, "Preparation and characterization of copper oxide nanofluid for heat transfer applications," Applied Nanoscience, vol. 4, no. 2, pp. 163-167, 2014/02/01 2014, doi: 10.1007/s13204-012-0184-7.

[39] Y.-P. Wu et al., "Temperature-Controlled Synthesis of Porous CuO Particles with Different Morphologies for Highly Sensitive Detection of Triethylamine," Crystal Growth & Design, vol. 17, no. 4, pp. 2158-2165, 2017/04/05 2017, doi: 10.1021/acs.cgd.7b00102.

[40] V. M. Faris, S. M. Hamad, A. A. Barzinjy, M. M. Khan, and D. Shaikhah, "Harvesting thermal energy with green-synthesised copper oxide/silver nanocomposites," International Journal of Sustainable Energy, vol. 44, no. 1, p. 2481969, 2025.

[41] S. M. Hamad, A. A. Barzinjy, R. Rafigh, P. Jalil, Y. Mirzaei, and D. Shaikhah, "Green Synthesis of ZnO/CuO Nanocomposites Using Parsley Extract for Potential In Vitro Anticoccidial Application," ACS Applied Bio Materials, vol. 6, no. 10, pp. 4190-4199, 2023/10/16 2023, doi: 10.1021/acsabm.3c00425.

[42] V. Gnielinski, "On heat transfer in tubes," International Journal of Heat and Mass Transfer, vol. 63, pp. 134-140, 2013/08/01/ 2013, doi: https://doi.org/10.1016/j.ijheatmasstransfer.2013.04.015.

[43] S. Z. Heris, M. Shokrgozar, S. Poorpharhang, M. Shanbedi, and S. H. Noie, "Experimental Study of Heat Transfer of a Car Radiator with CuO/Ethylene Glycol-Water as a Coolant," Journal of Dispersion Science and Technology, vol. 35, no. 5, pp. 677-684, 2014/05/04 2014, doi: 10.1080/01932691.2013.805301.

[44] D. K. Singh, D. K. Pandey, R. R. Yadav, and D. Singh, "A study of ZnO nanoparticles and ZnO-EG nanofluid," Journal of Experimental Nanoscience, vol. 8, no. 5, pp. 731-741, 2013/07/01 2013, doi: 10.1080/17458080.2011.602369.

[45] S. M. S. Murshed, K. C. Leong, and C. Yang, "Investigations of thermal conductivity and viscosity of nanofluids," International Journal of Thermal Sciences, vol. 47, no. 5, pp. 560-568, 2008/05/01/ 2008, doi: https://doi.org/10.1016/j.ijthermalsci.2007.05.004.

[46] S. Govindasamy, S. Harikrishnan, S. Kalaiselvam, H. Öztop, and N. Abu-Hamdeh, "Experimental investigation on the heat transfer performance of MHTHS using ethylene glycol-based nanofluids," Journal of Thermal Analysis and Calorimetry, vol. 143, 05/16 2020, doi: 10.1007/s10973-020-09764-y.

[47] J. C. Maxwell, "A treatise on electricity and magnetism, Clarendon," Oxford, vol. 314, p. 1873, 1881.

[48] A. H. Abdelaziz, W. M. El-Maghlany, A. Alaa El-Din, and M. A. Alnakeeb, "Mixed convection heat transfer utilizing Nanofluids, ionic Nanofluids, and hybrid nanofluids in a horizontal tube," Alexandria Engineering Journal, vol. 61, no. 12, pp. 9495-9508, 2022/12/01/ 2022, doi: https://doi.org/10.1016/j.aej.2022.03.001.

[49] Ç. Demirkır and H. Ertürk, "Convective heat transfer and pressure drop characteristics of graphene-water nanofluids in transitional flow," International Communications in Heat and Mass Transfer, vol. 121, p. 105092, 2021/02/01/ 2021, doi: https://doi.org/10.1016/j.icheatmasstransfer.2020.105092.

[50] S. Zeinali Heris, S. G. Etemad, and M. Nasr Esfahany, "Experimental investigation of oxide nanofluids laminar flow convective heat transfer," International Communications in Heat and Mass Transfer, vol. 33, no. 4, pp. 529-535, 2006/04/01/ 2006, doi: https://doi.org/10.1016/j.icheatmasstransfer.2006.01.005.

[51] S. Z. Heris, S. G. Etemad, and M. N. Esfahany, "Convective Heat Transfer of a Cu/Water Nanofluid Flowing Through a Circular Tube," Experimental Heat Transfer, vol. 22, no. 4, pp. 217-227, 2009/09/30 2009, doi: 10.1080/08916150902950145.

[52] V. Gnielinski, "New equations for heat and mass transfer in turbulent pipe and channel flow," International chemical engineering, vol. 16, no. 2, pp. 359-367, 1976.

[53] S. M. Ammar and C. W. Park, "Validation of the Gnielinski correlation for evaluation of heat transfer coefficient of enhanced tubes by non-linear regression model: An experimental study of absorption refrigeration system," International Communications in Heat and Mass Transfer, vol. 118, p. 104819, 2020/11/01/ 2020, doi: https://doi.org/10.1016/j.icheatmasstransfer.2020.104819.

[54] E. A. Mohamed, "Green synthesis of copper & copper oxide nanoparticles using the extract of seedless dates," Heliyon, vol. 6, no. 1, 2020, doi: 10.1016/j.heliyon.2019.e03123.

[55] E. Arulkumar, S. Thanikaikarasan, S. Rajkumar, and W. Wondimu, "Influence of solution pH dependency on structure, optical with photoelectrochemical characteristics of SILAR deposited copper oxide thin films," Heliyon, vol. 10, no. 13, 2024, doi: 10.1016/j.heliyon.2024.e33579.

[56] S. Omar and R. Mohammed, "BIOSYNTHESIS AND CHARACTERIZATION OF CuO NANOPARTICLES USING DIFFERENT pH," Science Journal of University of Zakho, vol. 11, 08/21 2023, doi: 10.25271/sjuoz.2023.11.3.1112.

[57] A. Raship, M. Z. Sahdan, F. Adriyanto, N. M. Fauzee, and A. S. Bakri, "THE EFFECTS OF PH VALUE ON THE PREPARATION OF COPPER OXIDE THIN FILMS BY DIP COATING TECHNIQUE," 2006.

[58] G. F. Aaga and S. T. Anshebo, "Green synthesis of highly efficient and stable copper oxide nanoparticles using an aqueous seed extract of Moringa stenopetala for sunlight-assisted catalytic degradation of Congo red and alizarin red s," Heliyon, vol. 9, no. 5, 2023, doi: 10.1016/j.heliyon.2023.e16067.

[59] A. S. Tijani and M. Y. Azreen Bin Mohd Yusoff, "Chapter Seven - Thermos-physical properties and heat transfer characteristic of copper oxide–based ethylene glycol/water as a coolant for car radiator," in Advanced Materials-Based Fluids for Thermal Systems, H. Muhammad Ali Ed.: Elsevier, 2024, pp. 169-186.

[60] A. Al Rafi, R. Haque, F. Sikandar, and M. N. Chowdhury, Experimental analysis of heat transfer with CuO, Al2O3/water-ethylene glycol nanofluids in automobile radiator. 2019, p. 040007.

[61] H. A. Kazem, M. T. Chaichan, and A. H. Al-Waeli, "Effect of CuO-water-ethylene glycol nanofluids on the performance of photovoltaic/thermal energy system: an experimental study," Energy Sources, Part A: Recovery, Utilization, and Environmental Effects, vol. 44, no. 2, pp. 3673-3691, 2022.

[62] S. K. Das, S. U. Choi, W. Yu, and T. Pradeep, Nanofluids: science and technology. John Wiley & Sons, 2007.

[63] Z. Mahmood, S. M. Eldin, A. F. Soliman, T. A. Assiri, U. Khan, and S. R. Mahmoud, "Impact of an effective Prandtl number model on the flow of nanofluids past an oblique stagnation point on a convective surface," Heliyon, vol. 9, no. 2, 2023, doi: 10.1016/j.heliyon.2023.e13224.

[64] M. F. Amran, S. M. Sultan, and C. P. Tso, "A Comprehensive Review of Mixed Convective Heat Transfer in Tubes and Ducts: Effects of Prandtl Number, Geometry, and Orientation," Processes, vol. 12, no. 12, p. 2749, 2024. [Online]. Available: https://www.mdpi.com/2227-9717/12/12/2749.

[65] G. Kalpana, K. R. Madhura, and R. B. Kudenatti, "Numerical study on the combined effects of Brownian motion and thermophoresis on an unsteady magnetohydrodynamics nanofluid boundary layer flow," Mathematics and Computers in Simulation, vol. 200, pp. 78-96, 2022/10/01/ 2022, doi: https://doi.org/10.1016/j.matcom.2022.04.010.